ISSN 1063-7834, Physics of the Solid State, 2018, Vol. 60, No. 9, pp. 1691–1697. © Pleiades Publishing, Ltd., 2018.
Original Russian Text © O.B. Romanova, S.S. Aplesnin, A.M. Khar'kov, V.V. Kretinin, A.M. Zhivul'ko, 2018, published in Fizika Tverdogo Tela, 2018, Vol. 60, No. 9, pp. 1650–1655.

SEMICONDUCTORS

Kinetic Properties of the $Mn_{1-x}Gd_xSe$ Solid Solutions

O. B. Romanova[b, *], S. S. Aplesnin[a, b], A. M. Khar'kov[a], V. V. Kretinin[a], and A. M. Zhivul'ko[c]

[a] *Siberian State University of Science and Technology, Krasnoyarsk, 660014 Russia*
[b] *Kirensky Institute of Physics, Federal Research Center "Krasnoyarsk Scientific Center," Russian Academy of Sciences, Siberian Branch, Krasnoyarsk, 660036 Russia*
[c] *Scientific and Practical Materials Science Center, National Academy of Science of Belarus, Minks, 220072 Belarus*
**e-mail: rob@iph.krasn.ru*

Received December 20, 2017; in final form, March 6, 2018

Abstract—The results of kinetic study of the $Mn_{1-x}Gd_xSe$ chalcogenide solid solutions with different substitute concentrations ($0 \le x \le 0.15$) in the temperature range of 80–400 K are reported. The difference between the Hall constant and thermopower signs has been found. The electron-type conductivity determined from the Hall constant and hysteresis of the I–V characteristics have been explained by the existence of nanoareas with local electric polarizations. The sharp extrema observed in the temperature dependence of thermopower are explained by splitting of a narrow 4f subband by the crystal field.

DOI: 10.1134/S1063783418090263

1. INTRODUCTION

The importance of studying chalcogenides is caused by their prospects for application in different fields of science and technology, including instrument engineering, quantum electronics, and laser spectroscopy. The uniqueness of these compounds consists, first of all, in the fact that they can have various types of magnetic ordering and electrical conductivity. The initial manganese monoselenide MnSe is an antiferromagnetic p-type semiconductor [1] and has a face-centered cubic (fcc) crystal structure of the NaCl type in the stable α modification. The band gap E_g of these compounds (2.0–2.5 eV) [1] was a decisive factor in choosing them as basic materials for electronics. According to neutron diffraction study, the magnetic phase transition temperature of the cubic manganese monoselenide is $T_N = 135$ K [2] and in the NiAs hexagonal phase, it coincides with the temperature of the structural transition $T_s = 272$ K [3]. In [4], we established the correlation between the electrical, structural, and magnetic properties of MnSe and a decrease in its resistivity in a magnetic field in the region of transition to the magnetically ordered state.

Cation substitution of 3d transition metals (e.g., chromium and cobalt) and 4f elements for manganese ions gives rise to new physical properties of the solid solutions, which are not observed in the initial compound [5–8]. Upon substitution of rare-earth (Gd) ions for manganese cations, additional exchange ferromagnetic interactions occur between manganese ions as a result of the s–d kinetic interaction and the degenerate electronic states arise in the d shell, which can be eliminated by the Jahn–Teller interaction or strong electron correlations and lead to the local electric polarization. If the values of hybridization of the d_{xz}–d_{xz} and d_{yz}–d_{yz} orbitals are lower than the splitting energy, the conductivity can be controlled by an external electric field. This effect will, most likely, manifest itself in measurements of the I–V characteristics. Electron doping changes not only the magnetic structure, but also the majority carrier sign.

Study of the kinetic properties of semiconductor materials is important in terms of obtaining information about the energy spectrum structure of carriers and their interaction with the crystal lattice [9]. It is well known that the thermopower is a sensitive kinetic property of a material. In most cases, in the trivalent rare-earth element chalcogenides, there is a discrepancy between the differential thermopower and Hall constant signs, which is explained by the carrier scattering mechanism and energy structure of the Brillouin zone. The competition of these two components leads to the difference between the signs [10].

The aim of this study was to investigate the effect of electron doping on the electronic structure and kinetic properties of the synthesized $Mn_{1-x}Gd_xSe$ chalcogenide solid solutions and establish the correlation between the Hall constant and thermopower.

2. EXPERIMENTAL

The $Mn_{1-x}Gd_xSe$ ($0 \le x \le 0.15$) solid solutions were prepared in a single-zone resistance furnace using the solid-state reaction from powders of the ini-

tial compounds placed in evacuated quartz ampoules [11, 12].

Phase composition and crystal structure of the $Mn_{1-x}Gd_xSe$ samples were determined at 300 K on a DRON-3 X-ray diffractometer (CuK_α radiation). Electrical resistivity, I–V characteristics, and thermopower were measured on the $Mn_{1-x}Gd_xSe$ samples with $x = 0.05$ and 0.15 in the form of parallelepipeds $5.00 \times 3.00 \times 8.00$ mm^3 in size. The dc electric measurements were performed by a four-probe method in the temperature range of 80–500 K. Strip silver contacts were formed on one of the sample surfaces at a distance of no smaller than 1 mm between them. The I–V characteristic was measured for 100 s; the sample heating was no more than one degree. The thermopower was measured by a two-probe method at the temperature difference of ~4–8 K between the probes. The Hall constant measurements were performed using a classical method on the samples with a pair of current contacts and a cross-shaped pair of potential Hall probes. In the experiment, contributions of spurious voltages induced by side galvano- and thermomagnetic effects were taken into account.

3. RESULTS AND DISCUSSION

According to the X-ray diffraction data, all the reflections in the X-ray diffraction pattern (Fig. 1) of the $Mn_{1-x}Gd_xSe$ ($x = 0.05$ and 0.15) solid solutions belong to a face-centered cubic (fcc) lattice of the NaCl type (sp. gr. $Fm3m$). The unit cell parameter increases with an increase in the substitute concentration from $a = 0.5460$ nm at $x = 0.05$ to $a = 0.5495$ nm at $x = 0.15$.

The synthesized $Mn_{1-x}Gd_xSe$ ($0 \le x \le 0.15$) compounds are antiferromagnets [13]. As the substitute concentration increases, the Neel temperature decreases from $T_N = 134$ K for initial MnSe to $T_N = 90$ K for the composition with $x = 0.15$ and the paramagnetic Curie temperature changes from $\Theta_p = -350$ K for initial MnSe to $\Theta_p = -90$ K for the composition with $x = 0.15$, which is indicative of the ferromagnetic exchange. The effective magnetic moment increases from $5.9\mu_B$ for MnSe to $6.29\mu_B$ for the composition with $x = 0.15$. Upon electron doping, the contribution to the magnetic moment is made by manganese ions with the multiplets characterized by the orbital angular momentum. For example, the degeneracy elimination in the t_{2g} subsystem induces the orbital magnetic moment and leads to the anisotropic electron density distribution and conductivity anisotropy. Current channels can be switched between the hybridized d_{xz}–d_{xz}, and d_{yz}–d_{yz} orbitals by an external electric field. This effect is reflected on in the thermoelectric properties of the $Mn_{1-x}Gd_xSe$ solid solution.

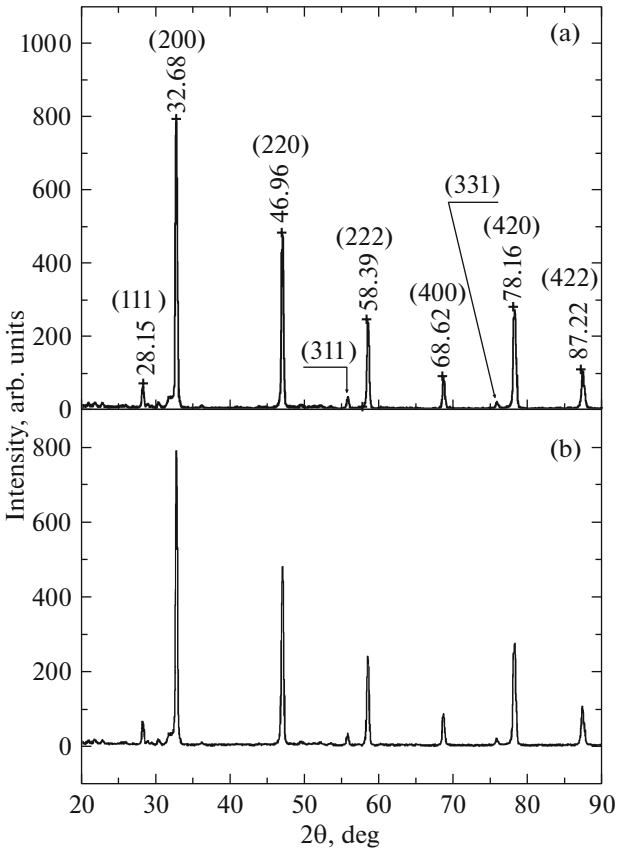

Fig. 1. X-ray diffraction patterns of the $Mn_{1-x}Gd_xSe$ samples with $x =$ (a) 0.05 and (b) 0.15.

Electron doping significantly affects the conducting and thermoelectric properties. The change in the conductivity type and electrical resistivity was observed. Figure 2 shows temperature dependences of the electrical resistivity for the compositions with $x = 0.05$ and 0.15. It should be noted that even at the low concentrations of substitution of ganglion ions for manganese ions, the resistivity increases over its value for the initial MnSe samples [4]. The temperature dependence of the electrical resistivity is typical of semiconductors with the activation energy determined from the slope of the straight portion of the $\log\rho(1/T)$ dependence, which decreases with an increase in the concentration from $\Delta E = 0.54$ eV ($x = 0.05$) to $\Delta E = 0.33$ eV ($x = 0.15$) in the temperature range of 290–400 K. The temperature behavior of the resistivity is indicative of the metal-type conductivity in the ranges of $T < 250$ K at $x = 0.15$ and $T < 190$ K at $x = 0.05$. Upon further heating, this portion changes for the semiconductor-type dependence. The changes in the temperature dependence of the resistivity are consistent with the Hall constant data and caused by a shift of the chemical potential relative to the $4f$ level.

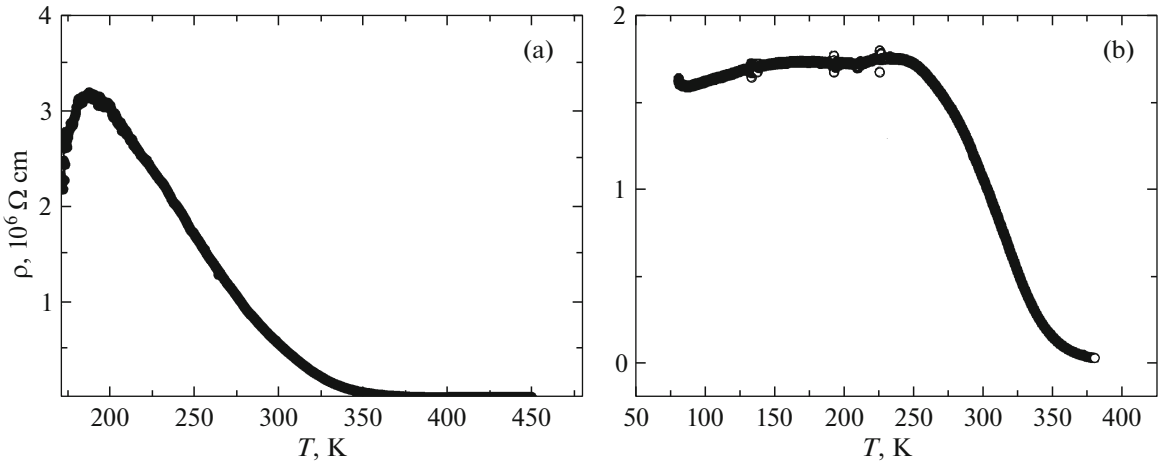

Fig. 2. Zero-field temperature dependences of the electrical resistivity for the $Mn_{1-x}Gd_xSe$ samples with x = (a) 0.05 and (b) 0.15.

The presence of inhomogeneous electronic states can be determined from the I–V characteristics. Figure 3 shows the I–V characteristics of the polycrystalline $Mn_{1-x}Gd_xSe$ samples with $x = 0.05$ and 0.15. The measurements were performed in the temperature range of 80–400 K. The samples with the low substitute concentration ($x = 0.05$) are characterized by the I–V hysteresis observed in a wide temperature range (80–360 K). The slight I–V hysteresis is also observed at $x = 0.15$, but only at $T > 300$ K. As the voltage increases, the current monotonically grows and the dependence contains an inflection point in the region of $U > 100$ V for both substitute concentrations, which vanishes with increasing temperature.

The sign of majority carriers and their mobility can be established from the Hall constant data. Figure 4 shows temperature dependences of the Hall constant for the $Mn_{1-x}Gd_xSe$ system with substitute concentrations of $x = 0.05$ and 0.15. The general regularity of the $R_H(T)$ dependences is the transition from the hole-type electrical conductivity typical of manganese monoselenide [4] to the electron-type one with an increase in the gadolinium ion concentration. For the composition with $x = 0.05$, the Hall constant is negative over the entire temperature range with a pronounced R_H minimum at $T = 200$ K, where the electron density at the chemical potential level is minimum (Fig. 4a). In this temperature range, electrons have the low mobility, which sharply grows above room temperature (inset in Fig. 4a). As the gadolinium ion concentration increases, the temperature of the minimum Hall constant shifts toward higher temperatures up to 320 K (Fig. 4b). The electron mobility for the composition with $x = 0.15$ starts growing above 200 K (inset in Fig. 4b). At the low gadolinium ion concentration ($x = 0.05$), the conductivity over the impurity electronic states is implemented. The electron transport occurs via temperature-activated hoppings with the activation energy calculated, in our case, from the temperature dependence of the mobility: $E_a = 0.03$ eV in the temperature range of 180–230 K and $E_a = 0.13$ eV in the temperature range of 270–360 K. The impurity conductivity is implemented via random diffusion and the mobility is expressed as [10] $\mu = \mu_0 \exp(-E_a/k_0T)$, where $\mu_0 = \frac{ea^2\nu}{k_0T}$, ν is the hopping frequency equal to the phonon frequency (~10^{13} Hz), and a is the distance between donors. As the impurity (gadolinium) concentration increases up to $x = 0.15$, the smooth transition from the impurity to band conductivity with an activation energy of $E_a = 0.3$ eV occurs.

The thermopower investigations allowed us to deeper understand the electronic processes occurring in the investigated $Mn_{1-x}Gd_xSe$ semiconductor system. Figure 5 shows temperature dependences of the thermopower. For both compositions, there are a sharp increase in the thermopower and the maxima of its absolute value at $T = 335$ K for $x = 0.05$ and $T = 273$ K for $x = 0.15$. These features are caused by splitting of the 4f level by the crystal field. The splitting value is $\Delta E = 50$–70 meV. The chemical potential is localized in the vicinity of the 4f-level energy and the contribution to the kinetic coefficients is caused by the electron density of states in the energy interval $\frac{\partial f(E)}{\partial T} \approx 2T$. Heating induces the electronic transitions between the 4f levels and the temperature difference at the ends of the sample leads to a shift in the chemical potential on one sample side and, consequently, to the difference between the carrier densities. The change in the thermopower sign at 373 K for $x = 0.05$ and at 298 K for $x = 0.15$ and the difference from the temperature

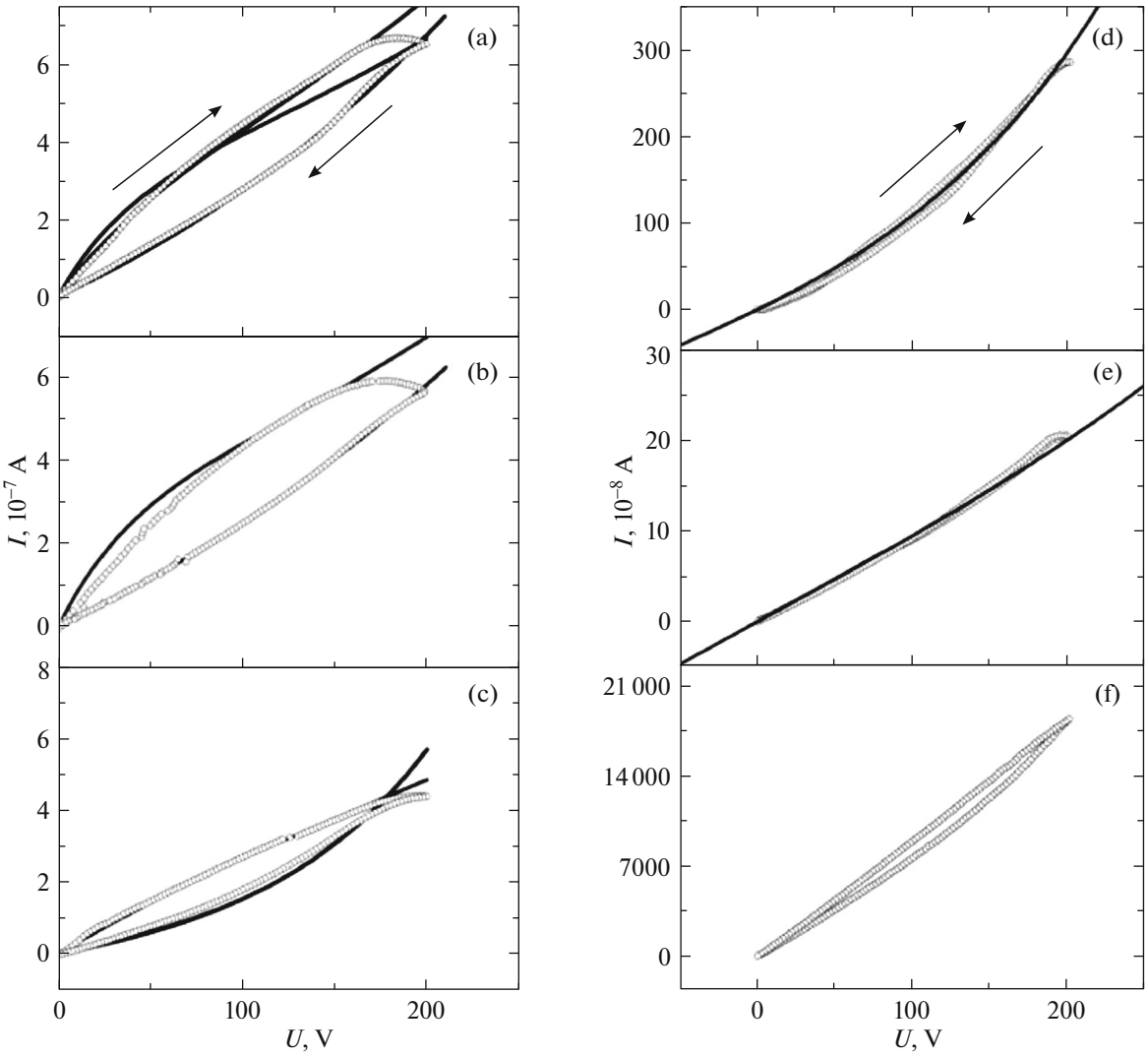

Fig. 3. Zero-field I–V characteristics of the $Mn_{0.95}Gd_{0.05}Se$ sample at temperatures of (a) 120, (b) 160, and (c) 360 K and the $Mn_{0.85}Gd_{0.15}Se$ sample at temperatures of (d) 80, (e) 200, and (f) 350 K. Lines show functional dependence (1).

behavior of the Hall constant is due to dragging electrons by phonons. As the gadolinium ion concentration increases, the 4*f*-subband width increases, the difference between the electron densities in the vicinity of the chemical potential decreases, and the thermoelectric efficiency drops by an order of magnitude.

4. MODEL

To explain the experimental results, we assume the electron from the gadolinium ion to pass to the 3*d* band of the nearest manganese ions, thereby inducing the orbital degeneracy, which is eliminated by the strong electron correlations [14] and leading to different types of orbital ordering or orbital glass [15, 16]. The electric polarization can be caused by the noncentrosymmetric overlap of the 3*d* and 5*d* electron orbitals or 4*f* orbital in the direction of the occupied orbitals. Thus, in the nanoarea where the gadolinium ion is only surrounded by the nearest manganese ions, the local symmetry is lowered and the electric polarization is induced.

The I–V hysteresis is caused by the existence of polar regions, where the polarization is randomly distributed in the $Mn_{1-x}Gd_xSe$ solid solutions. As the temperature increases, the polar regions with the polarization perpendicular to the current start rotating, which leads to an increase in the concentrations n_1 and n_2 with temperature (Table 1). The resulting field inside the sample $E = E_0 - \frac{P}{\varepsilon_0}$ decreases and the resistivity grows. We denote the concentrations of the polar

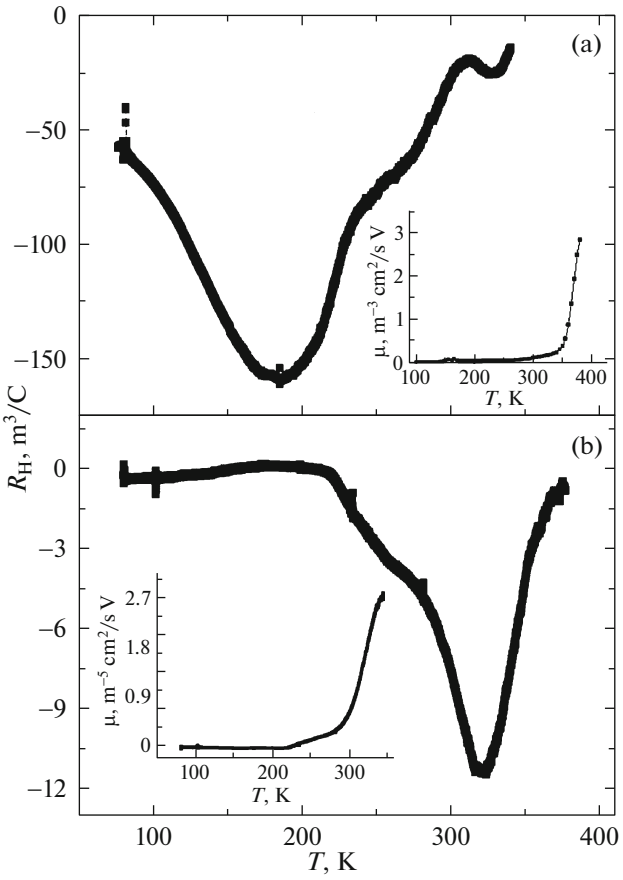

Fig. 4. Temperature dependences of the Hall constants for the $Mn_{1-x}Gd_xSe$ samples with x = (a) 0.05 and (b) 0.15. Inset: temperature dependences of mobility for the same samples.

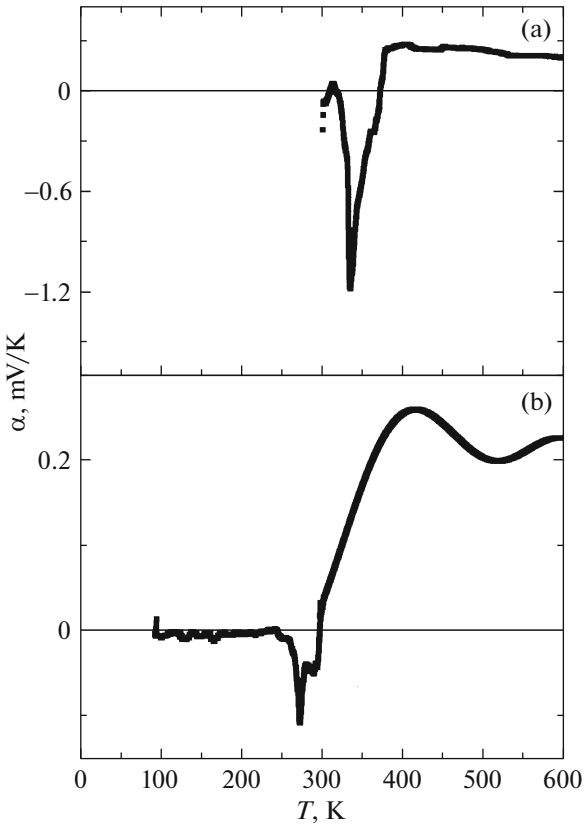

Fig. 5. Temperature dependence of the thermopower for the $Mn_{1-x}Gd_xSe$ samples with x = (a) 0.05 and (b) 0.15.

regions by n_1 and n_2. We present the voltage dependence of the current in the form

$$I = I_{01}\left(\exp\left(n_1\frac{eU}{kT}\right)-1\right) - I_{02}\left(\exp\left(-n_2\frac{eU}{kT}\right)-1\right), \quad (1)$$

where the currents $I_{01,\,02}$ change within (0.25–0.44) × 10^{-7} A and n_1 and n_2 are the fitting parameters.

The $I(U)$ functional dependence in Fig. 3 describes well the experimental data. The nanoareas form a glass with the degenerate states according to the electric dipole moment. The concentration of clusters with the opposite polarization directions sharply decreases. The fitting parameters for the I–V characteristic are given in Table 1. The electron density of states changes upon rotation of the polarization vectors with an increase in the cluster concentrations n_1 and n_2 [17]. For the composition with $x = 0.15$, the I–V characteristic is described by function (1) with the same cluster concentrations n_1 and n_2, which change with temperature.

The absolute values of the thermopower maxima (S) can be estimated using the Kubo–Greenwood formula [18]

$$S = \frac{1}{eT}\frac{L_{12}}{L_{11}} = \frac{eL^{12}}{T\sigma}, \quad (2)$$

$$L^{12} = \int \partial w\left(-\frac{\partial f(w)}{\partial w}\right)g^2(w)w, \quad (3)$$

where e is the elementary charge, T is the temperature, σ is the conductivity, g is the density of states, and f is the Fermi function. The electron density of the 4f-subband states can be presented in the form of two

Table 1. Fitting parameters for the I–V characteristics of $Gd_{0.05}Mn_{0.95}Se$

T, K	I_{01}	n_1	I_{02}	n_2
360	0.36	0.9	0.27	2.58
	0.66	4	0.26	4.8
160	0.36	0.54	0.27	4
	0.44	0.65	0.025	1.4
120	0.35	0.5	0.25	2.5
	0.45	0.5		0

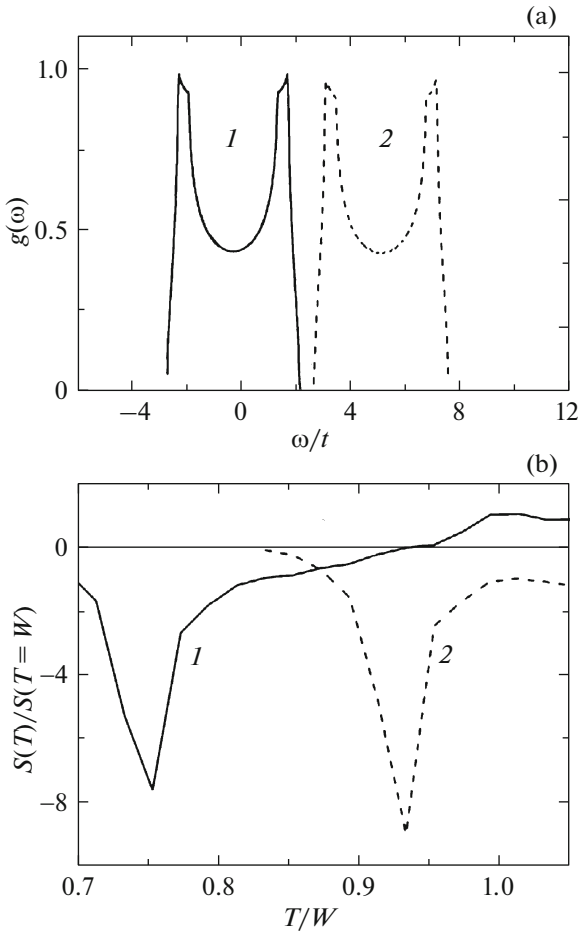

Fig. 6. (a) Seed density of the electronic states located (*1*) at the chemical potential level and (*2*) above it. (b) Relative thermopower $S(T)/S(T = W)$, where W is the 4*f*-subband width, as a function of normalized temperature T/W at (*1*, *2*) two densities of states.

maxima (Fig. 6). Let us consider two cases, when the chemical potential is located in the quasigap and below the density of electronic states. The calculated temperature dependences of the thermopower have sharp minima. The thermopower minimum shifts toward lower temperatures when the chemical potential shifts to the impurity subband. As the substitute concentration x increases, the chemical potential shifts relative to the f level. At $x = 0.05$, the 4*f* subband is located above the chemical potential and at $x = 0.15$, the subband broadens and the chemical potential hits the quasigap.

5. CONCLUSIONS

Thus, the kinetic properties of the $Mn_{1-x}Gd_xSe$ solid solutions at different substitute concentrations and temperatures were studied. Electron doping of the manganese chalcogenides changes the conductivity type from tunneling to activation with increasing temperature, which is accompanied by the growth of carrier mobility. The inflection points and hysteresis observed in the I–V characteristic were attributed to the presence of polar regions, where the polarization is randomly distributed in the investigated $Mn_{1-x}Gd_xSe$ solid solutions. The fitting parameters of the cluster concentration, which change with temperature, were presented. The general regularity of the temperature dependences of the Hall constant is the transition from the hole-type electrical conductivity typical of the initial manganese monoselenide to the electron-type one with increasing gadolinium ion concentration. The difference between the thermopower and Hall constant signs above room temperature related to dragging electrons by phonons was found. The sharp thermopower maxima induced by splitting of the 4*f*-subband of gadolinium ions by the crystal field were observed. The maximum thermopower was estimated using the Kubo–Greenwood formula.

ACKNOWLEDGMENTS

This study was supported by the Russian Foundation for Basic Research, project no. 18-52-00009 Bel_a and the state task no. 3.5743.2017/6.7.

REFERENCES

1. S. J. Youn, B. I. Min, and A. J. Freeman, Phys. Status Solidi B **241**, 1411 (2004).
2. G. I. Makovetskii and A. I. Galyas, Sov. Phys. Solid State **24**, 1558 (1982).
3. J. B. C. Efrem, D'Sa, P. A. Bhobe, K. R. Priolkar, A. Das, P. S. R. Krishna, P. R. Sarode, and R. B. Prabhu, J. Phys. **63**, 227 (2004).
4. S. S. Aplesnin, L. I. Ryabinkina, O. B. Romanova, D. A. Balaev, O. F. Demidenko, K. I. Yanushkevich, and N. S. Miroshnichenko, Phys. Solid State **49**, 2080 (2007).
5. S. S. Aplesnin, O. B. Romanova, K. I. Yashushkevich, and O. F. Demidenko, *Magnetic Phase Transitions and Kinetic Properties of 3d Metal Chalcogenides* (Sib. Gos. Aerokosm. Univ., Krasnoyarsk, 2017) [in Russian].
6. S. S. Aplesnin and M. N. Sitnikov, Phys. Solid State **58**, 1148 (2016).
7. A. I. Galyas, O. F. Demidenko, G. I. Makovetskii, K. I. Yanushkevich, L. I. Ryabinkina, and O. B. Romanova, Phys. Solid State **52**, 687 (2010).
8. S. S. Aplesnin, M. N. Sitnikov, O. B. Romanova, and V. V. Sokolov, Phys. Status Solidi B **253**, 1771 (2016).
9. B. M. Askerov, *Kinetic Effects in Semiconductors* (Nauka, Leningrad, 1970) [in Russian].
10. A. V. Golubkov, E. V. Goncharov, V. P. Zhuze, G. M. Loginov, V. M. Sergeeva, and I. A. Smirnov, *Physical Properties of Rare-Earth Element Chalcogenides* (Nauka, Leningrad, 1973) [in Russian].

11. S. Aplesnin, A. Galyas, O. Demidenko, G. Makovetskii, A. Panasevich, and K. Yanushkevich, Acta Phys. Polon. A **127**, 371 (2015).
12. O. B. Romanova, S. S. Aplesnin, A. M. Khar'kov, A. N. Masyugin, and K. I. Yanushkevich, Phys. Solid State **59**, 1314 (2017).
13. C. C. Aplesnin, M. N. Sitnicov, A. M. Panasevech, A. I. Galyas, O. F. Demidenko, and K. I. Yanushkevich, Bull. Russ. Acad. Sci.: Phys. **80**, 1306 (2016).
14. S. S. Aplesnin, L. I. Ryabinkina, G. M. Abramova, O. B. Romanova, A. M. Vorotynov, D. A. Velikanov, N. I. Kiselev, and A. D. Balaev, Phys. Rev. B **71**, 125204 (2005).
15. Y. Ren, T. T. M. Palstra, D. I. Khomskii, E. Pellegrin, A. A. Nugroho, A. A. Menovsky, and G. A. Sawatzky, Nature (London, U.K.) **396**, 441 (1998).
16. P. Khalifah, R. Osborn, Q. Huanq, H. W. Zandberqen, R. Jin, Y. Liu, D. Mandrus, and R. J. Cava, Science (Washington, DC, U. S.) **297**, 2237 (2002).
17. J.-S. Zhou and J. B. Goodenough, Phys. Rev. Lett. **96**, 247202 (2006).
18. K. Nagai, T. Momoi, and K. Kubo, J. Phys. Soc. Jpn. **69**, 1837 (2000).

Translated by E. Bondareva